**Supplementary Material**

# Structural transformations in the thermal dehydration of the $[Cu_2(bpa)(btec)(H_2O)_4]_n$ coordination polymer

**Laura Bravo-García, Edurne S. Larrea, Beñat Artetxe, Luis Lezama, Juan M. Gutiérrez-Zorrilla and Maria I. Arriortua**

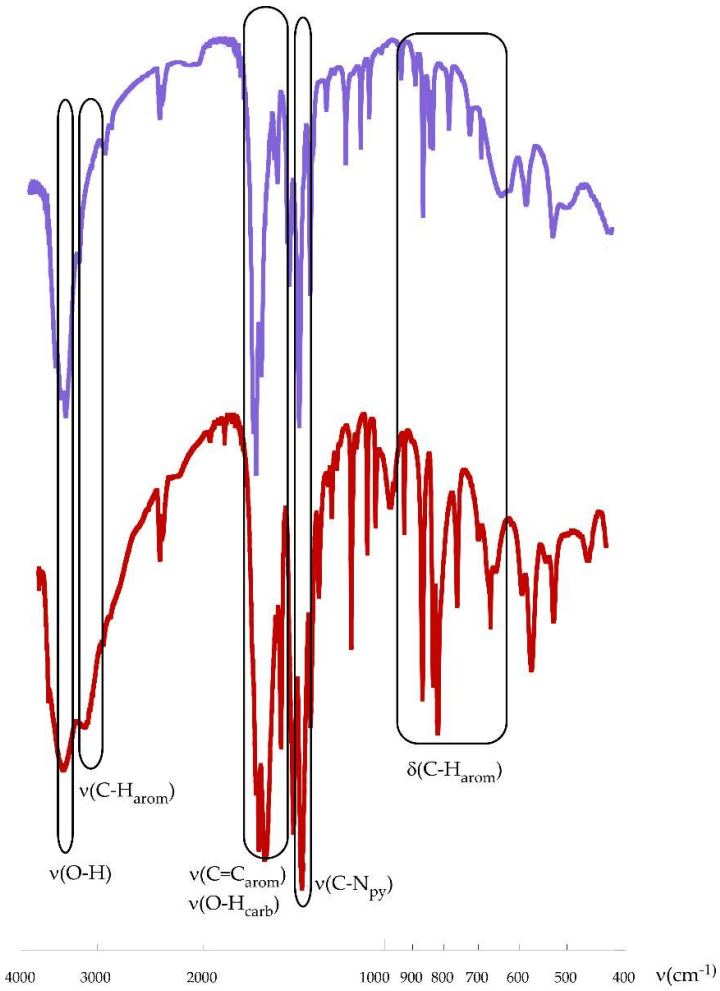


**Figure S1.** FT-IR spectrum of compound **1** and **1.ah**.

**Table S1.** Wavenumbers of the most intense bands in the IR spectra of **1** and **1.ah** together with their assignation.

| Assignation | Expected wave number | Compound 1 | Compound 1ah |
|---|---|---|---|
| ν(O-H) | 3650-3200 | 3430(m) | 3371(m) |
| $\nu(C\text{-}H_{aromatic})$ | 3150-3050 | 3082(w) | |
| $\nu(C{=}O_{carboxylic})$ | 1700-1600 | 1620(m) | 1625(s) |
| $\nu(C{=}C_{aromatic})$ | 1600, 1580, 1500, 1450 | 1600(s), 1580(s), 1490(m), 1410(s) | 1605(s), 1584(m), 1505 (w), 1462(m) |
| $\nu(C{=}N_{py})$ | 1300 | 1360(s) | 1359(s) |
| $\delta(C\text{-}H_{aromatic})$ | 950-650 | 890(m), 800(m), 770(m), 650(m) | 857(m), 836(m), 754(m), 672(m) |

Intensity: *s* = strong, *m* = medium *w*=weak, Vibrational modes: ν= stretching, δ= bending.

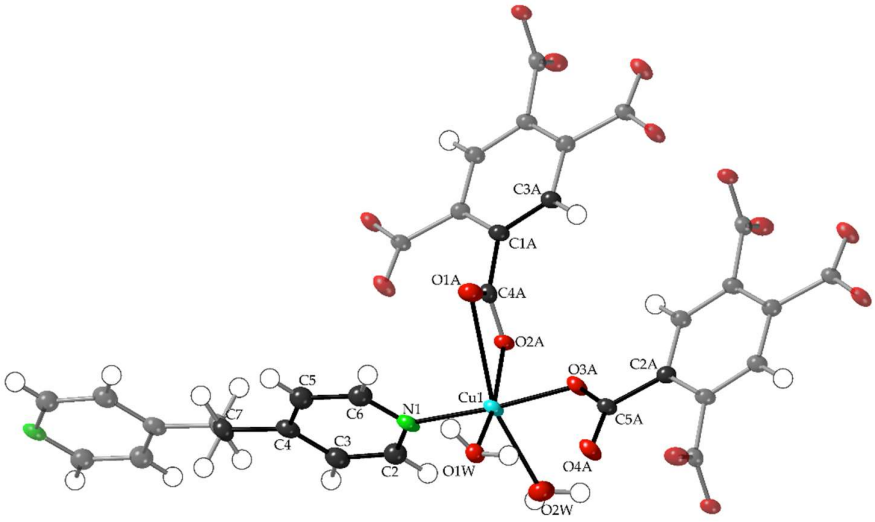


**Figure S2.** ORTEP[1] view of the coordination sphere of the copper (II) ion in $[Cu_2(bpa)(btec)(H_2O)_4]_n$, (**1**) showing 50% probability ellipsoids, together with atom labelling for the asymmetric unit.

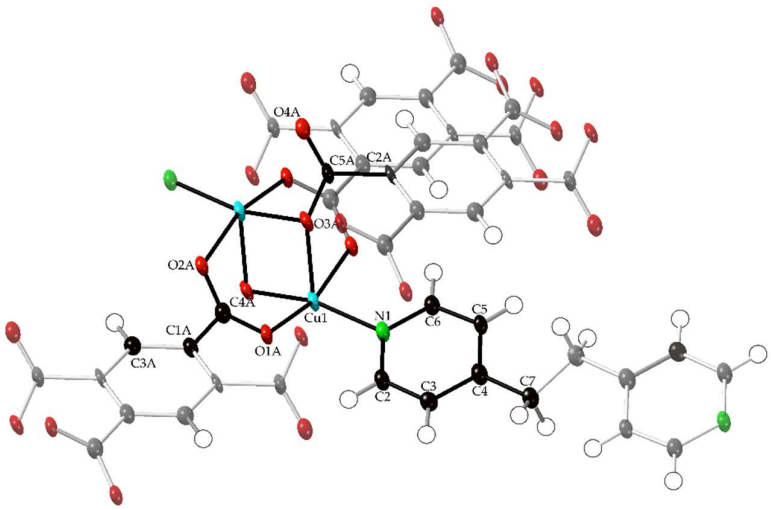


**Figure S3.** ORTEP[1] view of the copper (II) dimer in $[Cu_2(bpa)(btec)]_n$ (**1.ah**) showing 50% probability ellipsoids, together with atom labelling of the asymmetric unit. Only the ligands belonging to the coordination sphere of one of the copper (II) centers are shown for the sake of clarity.

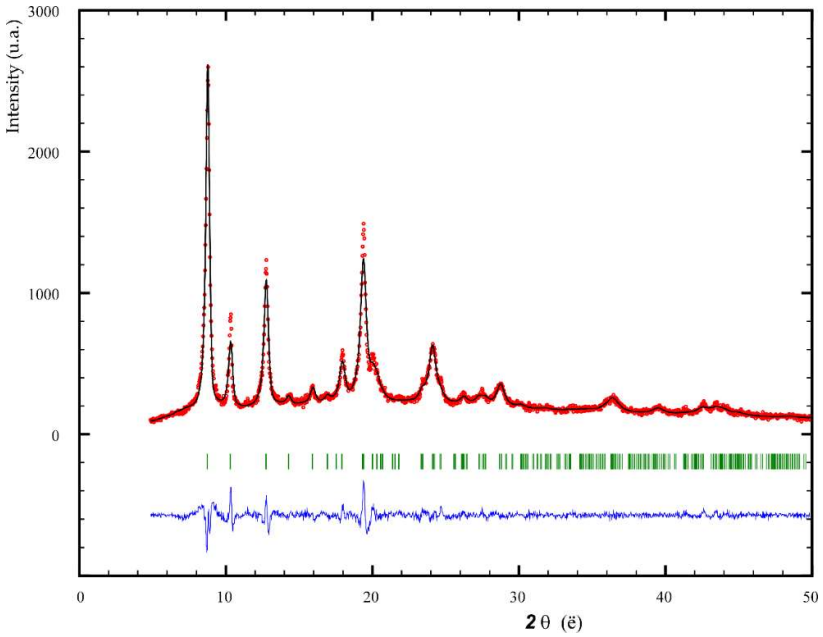


**Figure S4.** PXRD pattern-matching refinement plot of **1** after being heated at 200°C, using the cell unit parameters of **1.ah**.

**Table S2.** Cell parameters and agreement factors obtained in the pattern-matching procedure performed on **1** heated at 200 °C.

| | | | |
|---|---|---|---|
| $a$ (Å) | 5.6691 | $\alpha$ (°) | 95.601 |
| $b$ (Å) | 8.6899 | $\beta$ (°) | 98.381 |
| $c$ (Å) | 10.2963 | $\gamma$ (°) | 95.884 |
| $V$(Å$^3$) | 495.8978 | $\chi^2$ | 1.62 |
| $R_b$ | 6.08 | $R_p$ | 7.80 |

[a] $R_b = 100(\sum_h |I_{obs.h} - I_{cal.h}|)/(\sum_h |I_{obs.h}|)$ ; $R_p = 100(\sum_{i=l,n} |Y_i - Y_{c,i}|)/(\sum_{i=l,n} y_i)$ ; $\chi^2 = [R_{wp}/R_{exp}]^2$

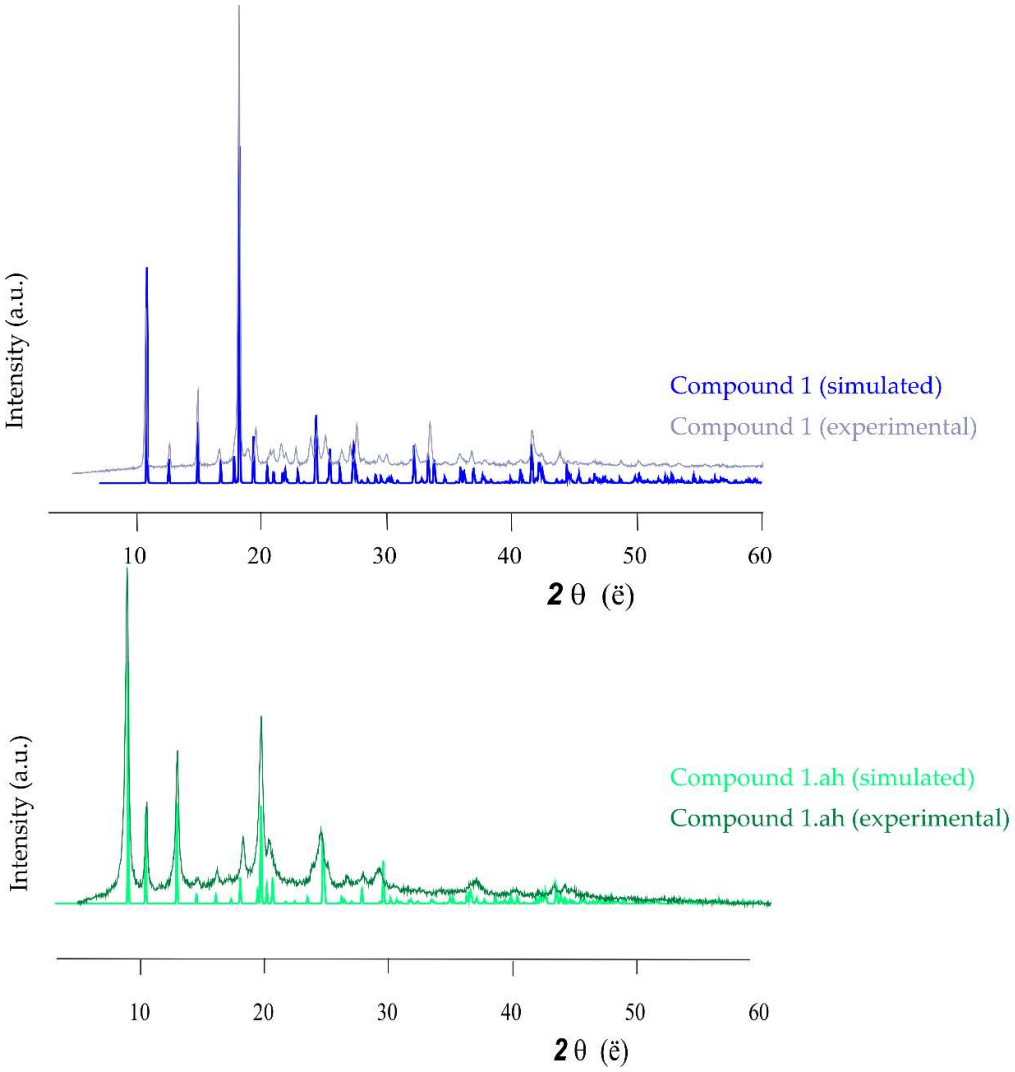


**Figure S5.** Comparison between experimental and simulated PXRD patterns for compounds **1** and **1.ah**.

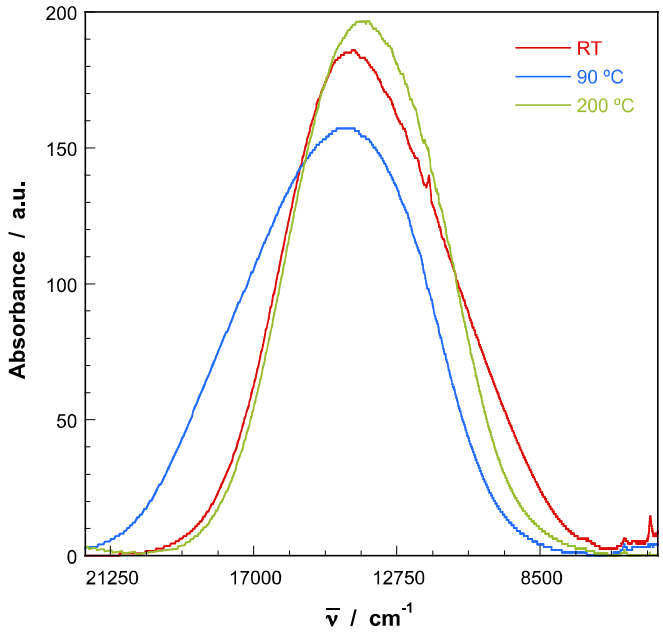


**Figure S6.** Diffuse reflectance spectra recorded at room temperature on polycristalline samples of **1** and the corresponding dehydrated phases.

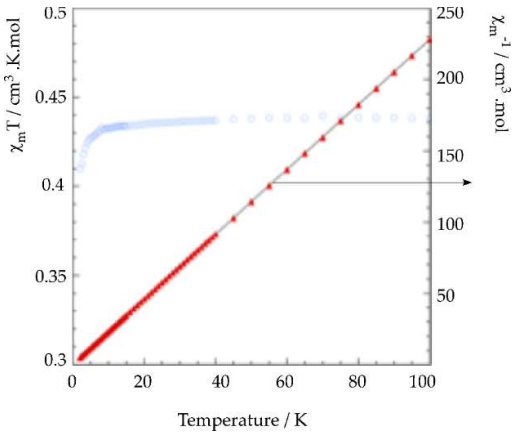


**Figure S7.** Thermal evolution of $1/\chi_m$ (red triangles) and $\chi_m T$ product (blue circles) for **1**. Fit of the magnetic susceptibility data to the Curie-Weiss law (black solid line)

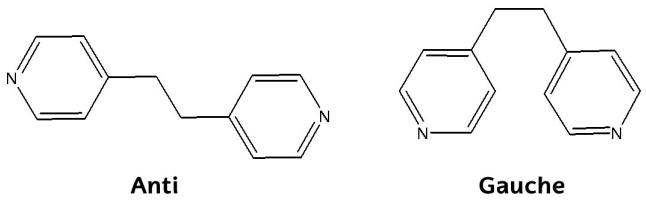


**Figure S8.** Molecular structures of different extreme conformations (*anti* and *gauche*) for the *bpa* ligand.

**REFERENCES:** [1] Farrugia, L.J. ORTEP-3 for windows - a version of ORTEP-III with a graphical user interface (GUI). *J. Appl. Crystallogr.* **1997,** *30,* 565.